

## STRANGENESS MEASUREMENTS WITH HADES\*

ROLAND KOTTE

for the HADES Collaboration

Helmholtz-Zentrum Dresden-Rossendorf, Institut für Strahlenphysik  
P.O. Box 510119, 01314 Dresden, Germany*(Received November 15, 2011)*

We present strangeness data taken with the High Acceptance Di-Electron Spectrometer (HADES) at the SchwerIonenSynchrotron SIS18 at the GSI Helmholtzzentrum Darmstadt. HADES, primarily designed to measure dielectrons, offers excellent hadron identification capabilities, too. Yields and phase-space distributions have been determined for the collision system Ar+KCl at 1.76A GeV and for strange particle species, with a substantial number of them being produced well below the production threshold in elementary nucleon–nucleon collisions. Here, sub-threshold production of  $\phi$  mesons appeared to contribute substantially to the  $K^-$  yield. Confronting the  $K_S^0$  spectra, measured over a wide range in momentum and rapidity, to predictions of the IQMD transport model points to a repulsive in-medium  $K^0$  potential of about 40 MeV. Furthermore, we present our results on  $\Lambda$ - $p$  intensity interferometry in Ar+KCl and compare them to other data.

DOI:10.5506/APhysPolB.43.601

PACS numbers: 25.75.-q, 25.75.Dw, 25.75.Gz, 25.70.Pq

**1. Introduction**

Originally, the HADES spectrometer [1] at SIS18, GSI Darmstadt, is aimed at the investigation of dielectrons [2] produced in heavy-ion collisions at energies of about 1–2A GeV. In the late nineties the DLS Collaboration reported on an excess of  $e^+e^-$  pairs in the region of low invariant masses, *i.e.* between the pion and  $\eta$  masses [3]. This excess could not be explained by model calculations (*e.g.* [4]) for a rather long time. Only a decade later, the ‘DLS-puzzle’ could be solved. The DLS data were confirmed by

---

\* Presented at the Conference “Strangeness in Quark Matter 2011”, Kraków, Poland, September 18–24, 2011.

HADES [5] and the dielectron production in C+C collisions could be explained as a superposition of elementary reactions [6]. Nevertheless, in the aforementioned intermediate-mass range an excess of about a factor of three over the elementary reference was found for collisions of a slightly larger system, Ar+KCl [7]. This finding suggests the onset of nontrivial effects of the ambient nuclear medium acting onto the decay of short-lived baryonic resonances (*e.g.*  $\Delta(1232)$ ). An even stronger excess is expected for large systems (as Au+Au, to be measured by HADES in 2012), where in central collisions and at maximum SIS energies densities of 2–3 times nuclear ground state density could be reached. Though the investigation of dilepton production is the main topic of HADES, the apparatus is well suited for the study of strange hadrons, too. In the following, a few examples will demonstrate this fact.

## 2. Strangeness measurements with HADES

### 2.1. Strangeness production near and below threshold

HADES is capable to identify particles carrying strangeness, either directly via the dependences of the specific energy loss of charged particles and/or the Time of Flight *vs.* momentum, the latter one being derived from the deflection of charged particles in the magnetic field ( $K^+$ ,  $K^-$ ,  $\phi \rightarrow K^+K^-$  [8]), or via the weak decay into charged particles involving topological cuts ( $K_S^0 \rightarrow \pi^+\pi^-$  [9],  $\Lambda \rightarrow p\pi^-$  [10],  $\Xi^- \rightarrow \Lambda\pi^- \rightarrow p\pi^-\pi^-$  [11]). The deduced  $K^+$ ,  $K^-$  rapidity distributions (Fig. 1, left panel) are found systematically wider than simulated ones assuming isotropic thermal emission, an observation found for  $\Lambda$  hyperons, too (see below). The yield of  $\phi$  mesons appears surprisingly large. Hence, about  $18 \pm 7\%$  of the  $K^-$  mesons arise from  $\phi$  decays [8]. Due to the decay kinematics, the  $K^-$  spectral are substantially softened [13]. The yields and spectral distributions of  $K^+$ ,  $K^-$ , and  $\phi$  mesons could be well reproduced with a Boltzmann–Ühling–Uhlenbeck transport approach [14].

We studied in-medium effects on  $K^0$  mesons in Ar+KCl collisions at 1.76A GeV taking advantage of the good acceptance of HADES at low transverse momentum [9]. In Fig. 2, we compare the experimental  $p_t$  distributions for different rapidity bins with the corresponding results by the IQMD transport approach [12] with (dashed curves) and without (dotted curves) taking into account a repulsive  $K^0$ -nucleus potential. For all rapidity bins, but most evidently at mid-rapidity ( $y_{c.m.} = y - y(c.m.) = 0$ ), the output of the model version which includes the repulsive potential agrees with the HADES results, while the calculations without such potential clearly fail to reproduce the experimental data. Our  $K_S^0$  data suggest a repulsive in-medium  $K^0$  potential of about 40 MeV strength.

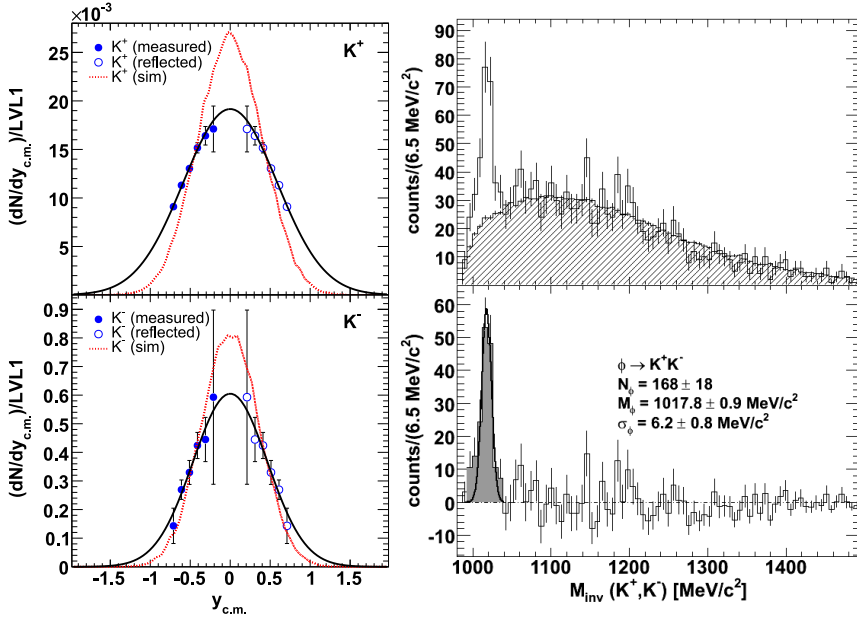


Fig. 1. Left: Rapidity density distributions of  $K^+$  (top) and  $K^-$  mesons (bottom). The full symbols show the measured data whereas the open ones are reflected data with respect to the c.m. rapidity. The curves represent Gaussian fits to the data. The overlaid dotted lines are simulated isotropic thermal distributions which have been normalized to the integral yield of the experimental data. Right: The invariant-mass distribution of  $K^+ - K^-$  pairs (top panel). The combinatorial background (shaded area) is obtained by the mixed-event technique. The background-subtracted distribution with the  $\phi$  meson signal (grey area with a Gaussian fit) is given on the bottom panel.

$\Lambda$  hyperons have been investigated in Ar+KCl collisions at 1.76A GeV [10]. Figure 3 represents some results. As for charged kaons, we find the width of  $\Lambda$  rapidity distribution (left panel) being significantly larger than that ( $FWHM_y \simeq 0.7$ ) expected from the mid-rapidity value,  $T_{\text{eff}} \simeq 95$  MeV, of the inverse slope parameter  $T_B(y)$  (right panel) of thermally distributed particles, suggesting partial transparency of small collision systems, in accordance with the stopping systematics reported by the FOPI Collaboration for the SIS18 energy regime [15, 16].

The high resolution of HADES for the selection of secondary vertices arising from weak decays and the high statistics accumulated for the collision system Ar+KCl at 1.76A GeV allowed to investigate the deep-threshold production ( $\sqrt{s_{NN}} - \sqrt{s_{\text{thr}}} = -640$  MeV) of the double-strange  $\Xi^-$  hyperon [11]. Figure 4 shows the results. The reconstructed signal is significantly larger

than any available model prediction. This calls for a better understanding of strangeness-exchange reactions, conjectured to be the dominant process for  $\Xi^-$  production below and close to threshold.

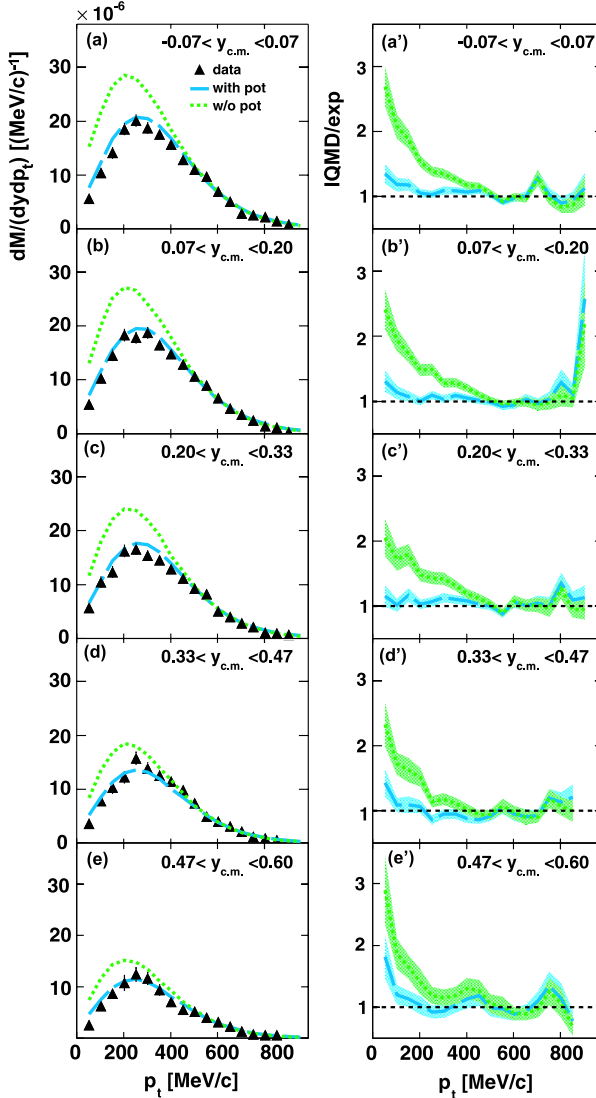


Fig. 2. Left panels:  $p_t$  distribution of the experimental  $K_S^0$  data (full triangles) together with the yields calculated by the IQMD model including a repulsive  $K^0$ -nucleus potential of 46 MeV (dashed curves) and without potential (dotted curves) for different rapidity bins. Right panels: Ratio between the calculation by the IQMD model and the experimental data as a function of  $p_t$  for different rapidity bins.

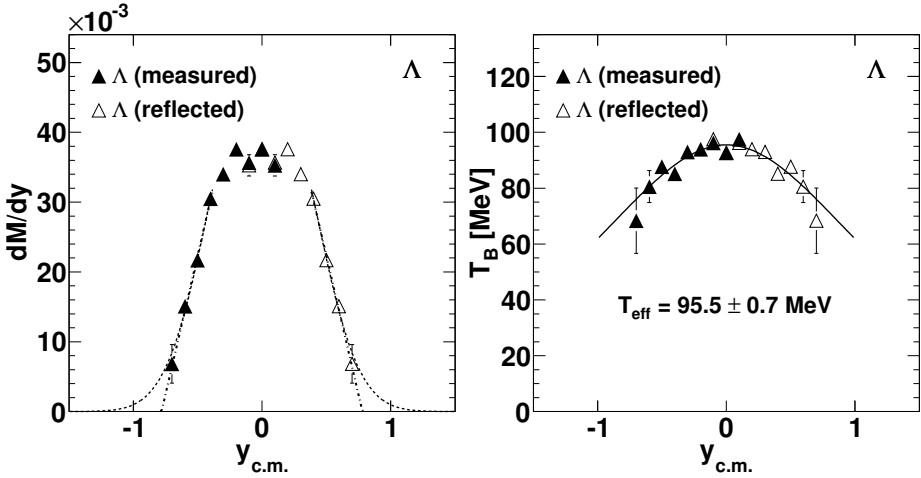


Fig. 3. The rapidity density distribution (left panel) and the dependence on rapidity of the inverse-slope parameter (right panel) as derived from the transverse-mass spectra of  $\Lambda$  hyperons in Ar+KCl collisions at 1.76A GeV [10]. The full curve represents the dependence  $T_B(y_{c.m.}) = T_{eff} / \cosh(y_{c.m.})$  for a Maxwell-Boltzmann distribution.

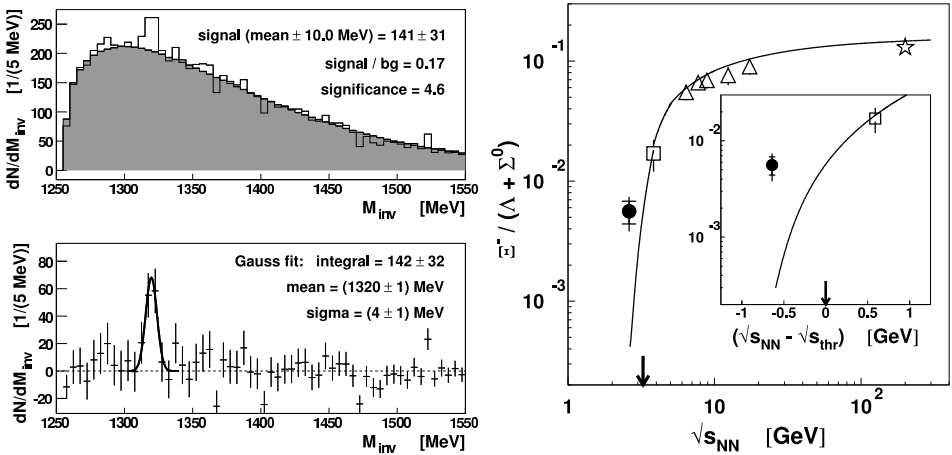


Fig. 4. Left: The invariant-mass distribution of  $\Lambda\pi^-$  pairs in Ar+KCl collisions at 1.76A GeV together with the combinatorial background (grey-shaded histogram) generated by mixed-event technique (upper panel) and the  $\Xi^-$  signal after background subtraction (lower panel). Right: The excitation function of the  $\Xi^- / (\Lambda + \Sigma^0)$  ratio [11].

## 2.2. Femtoscopy involving strange particles

The HADES result of  $\Lambda p$  intensity interferometry [17], *i.e.* the  $\Lambda p$  correlation function after close-track and purity corrections, is displayed in Fig. 5 (left panel) with a fit function derived from [18]. Following the procedure described in [19], we used the  $\Lambda p$  scattering lengths ( $f_0^s = -2.88$  fm,  $f_0^t = -1.66$  fm) and effective ranges ( $d_0^s = 2.92$  fm,  $d_0^t = 3.78$  fm) for the spin singlet and triplet states of the  $\Lambda p$  system as given in [20]. The optimum Gaussian radius provided by the fit amounts to  $r_0 = (2.09 \pm 0.16^{+0.12+0.09+0.09}_{-0.10-0.16-0.11})$  fm, where the 1st error is the statistical error, while the 2nd, 3rd, and 4th ones represent the systematic errors due to the uncertainties of the close-track correction with embedded  $\Lambda$ s, due to the pair purity correction, and due to a  $\pm 25\%$  variation of the scattering lengths entering the model [18], respectively. On the right panel of Fig. 5 the Gaussian  $\Lambda p$  radius is compared to similar radii derived by other experiments. Here, we show the Gaussian radius as a function of the number of participants to the power of one-third,  $A_{\text{part}}^{1/3}$ , which is calculated from the centrality and the total size of the corresponding collision system using a geometrical model of penetrating sharp spheres. While for the data measured by NA49 [21] at SPS (158A GeV Pb+Pb), by STAR [19] at RHIC (Au+Au at  $\sqrt{s_{NN}} = 200$  GeV), and by CLAS [22] at JLab (preliminary results from

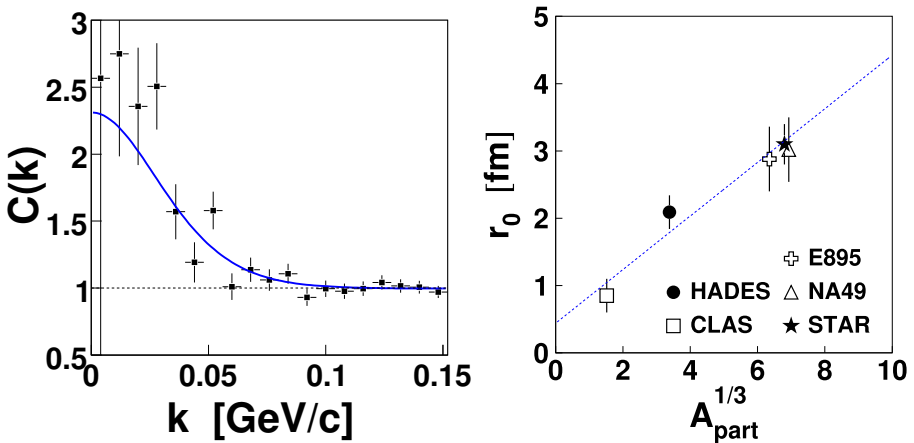


Fig. 5. Left: The  $\Lambda p$  correlation function as a function of the momentum in the pair rest frame [17]. The full curve represents the best fit with the Analytical Model by Lednicky and Lyuboshitz [18]. Right: The Gaussian radius of the  $\Lambda p$  emission source as a function of system size. The symbols indicate data taken with HADES at SIS, CLAS [22] at JLab, E895 [23] at AGS, NA49 [21] at SPS, and STAR [19] at RHIC, respectively. The dashed line is a linear regression to the data.

$e+^3\text{He}$  ( $^4\text{He}$ ) at 4.7 (4.46) GeV), the Gaussian radius  $r_0$  is determined using the same model as in the present analysis, the half-maximum radius  $R_{1/2}$  derived by E895 [23] at AGS (6A GeV Au+Au) applying an imaging procedure was transformed to a Gaussian radius via  $r_0 = R_{1/2}/\sqrt{4\ln 2}$ . Clearly, the  $A_p$  source radius increases with system size. Similarly to our results on the system-size dependence of  $pp$  correlation radii [24] (including data by the FOPI Collaboration [25]) and to the systematic trends of two-pion [26, 27] and two-kaon [28] source radii, we find an almost linear increase with the cube root of the number of participants. Hence, the correlation radius is a good measure of the system size.

### 3. Summary

In summary, we investigated various observables of hadrons involving strangeness. The data are taken with the dielectron spectrometer HADES. We showed that HADES is well suited not only to access the leptonic but also the hadronic channels with high precision. Single-particle quantities, two- and three-particle correlations of charged hadrons are presented, allowing to contribute to highly topical discussions, *e.g.* on modifications of hadronic properties in an ambient nuclear medium.

### REFERENCES

- [1] G. Agakichiev *et al.* [HADES Collaboration], *Eur. Phys. J.* **A41**, 243 (2009).
- [2] G. Agakichiev *et al.* [HADES Collaboration], *Phys. Rev. Lett.* **98**, 052302 (2007).
- [3] R.J. Porter *et al.* [DLS Collaboration], *Phys. Rev. Lett.* **79**, 1229 (1997).
- [4] E.L. Bratkovskaya, C.M. Ko, *Phys. Lett.* **B445**, 265 (1999).
- [5] G. Agakishiev *et al.* [HADES Collaboration], *Phys. Lett.* **B663**, 43 (2008).
- [6] G. Agakichiev *et al.* [HADES Collaboration], *Phys. Lett.* **B690**, 118 (2010).
- [7] G. Agakishiev *et al.* [HADES Collaboration], *Phys. Rev.* **C84**, 014902 (2011).
- [8] G. Agakishiev *et al.* [HADES Collaboration], *Phys. Rev.* **C80**, 025209 (2009).
- [9] G. Agakishiev *et al.* [HADES Collaboration], *Phys. Rev.* **C82**, 044907 (2010).
- [10] G. Agakishiev *et al.* [HADES Collaboration], *Eur. Phys. J.* **A47**, 21 (2011).
- [11] G. Agakishiev *et al.* [HADES Collaboration], *Phys. Rev. Lett.* **103**, 132301 (2009).
- [12] C. Hartnack *et al.*, *Eur. Phys. J.* **A1**, 151 (1998).
- [13] M. Lorenz [HADES Collaboration], *PoS (BORMIO2010)*, 038 (2010).
- [14] H. Schade, Gy. Wolf, B. Kämpfer, *Phys. Rev.* **C81**, 034902 (2010).
- [15] W. Reisdorf *et al.* [FOPI Collaboration], *Phys. Rev. Lett.* **92**, 232301 (2004).

- [16] W. Reisdorf *et al.* [FOPI Collaboration], *Nucl. Phys.* **A848**, 366 (2010).
- [17] G. Agakishiev *et al.* [HADES Collaboration], *Phys. Rev.* **C82**, 021901 (2010).
- [18] R. Lednicky, V.L. Lyuboshitz, *Sov. J. Nucl. Phys.* **35**, 770 (1982);  
V.L. Lyuboshitz, *Sov. J. Nucl. Phys.* **48**, 956 (1988).
- [19] J. Adams *et al.* [STAR Collaboration], *Phys. Rev.* **C74**, 064906 (2006).
- [20] F. Wang, S. Pratt, *Phys. Rev. Lett.* **83**, 3138 (1999).
- [21] T. Anticic *et al.* [NA49 Collaboration], *Phys. Rev.* **C83**, 054906 (2011).
- [22] K.R. Mikhailov *et al.* [CLAS Collaboration], *Phys. At. Nucl.* **72**, 668 (2009);  
*Acta Phys. Pol. B* **40**, 1171 (2009).
- [23] P. Chung *et al.* [E895 Collaboration], *Phys. Rev. Lett.* **91**, 162301 (2003).
- [24] G. Agakishiev *et al.* [HADES Collaboration], *Eur. Phys. J.* **A47**, 63 (2011).
- [25] R. Kotte *et al.* [FOPI Collaboration], *Eur. Phys. J.* **A23**, 271 (2005).
- [26] M.A. Lisa, S. Pratt, R. Soltz, U. Wiedemann, *Annu. Rev. Nucl. Part. Sci.* **55**, 357 (2005).
- [27] S.S. Adler *et al.* [PHENIX Collaboration], *Phys. Rev. Lett.* **93**, 152302 (2004).
- [28] S. Afanasiev *et al.* [PHENIX Collaboration], *Phys. Rev. Lett.* **103**, 142301 (2009).